GEOMETRIC CHARACTERIZATION OF A TARGET ABOVE THE HALF-SPACE INTERFACE USING SUPPORT VECTOR MACHINE

Chao Li, Si-Yuan He ,Guo-Qing Yin and Guo-Qiang Zhu
School of Electronic Information, Wuhan University, Wuhan, China

Keywords: Support Vector Machine, Inverse Scattering, Composite Model, Multilevel UV Method.

Abstract: The geometric parameters of a electrically large square above a rough surface are reconstructed by means of support vector machine (SVM). The SVM input data are the amplitude of backscattered electric fields obtained from the accurate and efficient EM numerical simulation. The aim of our research is to reconstruct the geometric information while using computational resources as reduced as possible. Therefore, how the spatial and frequency diversity affect the reconstruction is analysed with respect to the characteristics of the scattered fields. Numerical experiments show that it is feasible to get an accurate reconstruction result with the backscattered multi-frequency data collected at just a few observation points which are specially selected based on scattering characteristics.

1 INTRODUCTION

Both the scattering and the inverse scattering from a target above the half-space interface have a broad range of applications, such as target identification and microwave remote sensing (Ye and Jin, 2006; Deng et al., 2010).

The electromagnetic (EM) inverse scattering is to recover some unknown information of the scattering model through scattered fields probed at the observation points where antennas are placed (Bermani et al., 2002; Persico et al., 2005; Caorsi et al., 2005; Qing, 2003). Compared with a target in the free space, the inverse scattering from a target above a rough surface is much more difficult because of the complicated multiple-interactions between the target and rough surface. In recent years, neural networks (NN) and support vector machine (SVM) are proposed to solve EM inverse problems. In particular, as far as buried objects investigations are concerned, NNs have been applied to face the problem in the frequency/time domain (Bermani et al., 2002; Pettinelli et al., 2009), while SVM is used to deal with the buried objects detection (Caorsi et al., 2005).

In the following, how the spatial and frequency diversity affect the reconstruction is analyzed in terms of electrically large objects by analyzing the characteristics of the scattered field. In the end, the side length and height of a two-dimensional electrically large square above a rough surface are successfully reconstructed from the backscattered electric fields with the backscattered multifrequency data collected at just a few observation points (practically more convenient).

2 INVERSE PROBLEM

The geometry of the problem is shown in Figure 1, a 2-D PEC square with unknown side length L is located at a certain height of H above a PEC rough surface, which is generated with the Pierson-Moskowitz (P-M) spectrum. A truncation of the rough surface is required and a tapered wave is

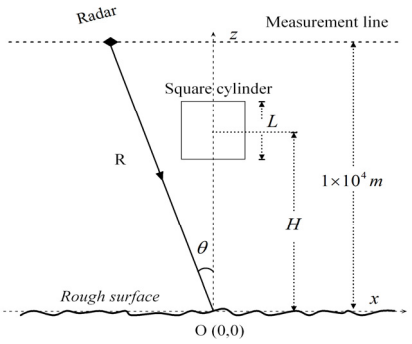

Figure 1: Geometry of the inverse problem.

352 Li C., He S., Yin G. and Zhu G..
GEOMETRIC CHARACTERIZATION OF A TARGET ABOVE THE HALF-SPACE INTERFACE USING SUPPORT VECTOR MACHINE .
DOI: 10.5220/0003722403520355
In *Proceedings of the International Conference on Evolutionary Computation Theory and Applications* (ECTA-2011), pages 352-355
ISBN: 978-989-8425-83-6

incident to avoid scattering effects from surface edges (Ye and Jin, 2006). A TM polarized (with electric field in y direction) tapered wave E_i is used to illuminate the composite model with the incident angle θ. Suppose R is the distance between the radar and the reference point O.

The inverse problem considered is to reconstruct the geometric parameters of the target, such as the side length and the height, from the backscattered electric fields. Mathematically, the problem reduces to determine the following relation:

$$\boldsymbol{L} = \phi(\boldsymbol{E}^s) \quad (1)$$

where $\boldsymbol{E}^s$ is the scattered electric field array.

In the previous study, in order to get an exhaustive information, many observation points are set equally spaced on a measurement line to gather the backscattered fields. In this paper, we consider an efficient multifrequency–singleview-monostatic det- ection way and the objects under study are electric- ally large. How the spatial diversity and frequency diversity affect the reconstruction is analyzed.

3 NUMERICAL RESULTS

3.1 Traditional Case

In this section, we firstly reconstruct the side length of a square above a rough surface using the singlefrequency–multiview–monostatic configurati- on, i.e., a measurement configuration wherein the transmitter and the receiver are placed together at 21 equally spaced positions along the measurement line. The incident wave is operating at 300MHz with the freespace wavelength $\lambda = 1(m)$. The training sampl- es are $L = 4.01 + 0.1i\ (m), i = 0, \cdots 9$ while the test samples are $L = 4.045 + 0.1i\ (m),\ i = 0 \cdots 8$. Wind spe- ed U is $0m/s$. The errors are quantified by the following formula: $RelErr(p) = | p_t - p_r | / | p_t | \times 100$, Where p is the considered unknown variable, subscript t and r indicate the real value and the reconstructed value of the variable respectively. The average error is 2.0%.

Then, we use the multifrequency-singleview-monostatic configuration. In this case, the incident angle is $\theta = 0^\circ$. The training and test sets are the same as we used above. The frequencies are chosen according to the rule: $f = 300 + 10i\ (MHz), i = 0 \cdots 9$. The average error is 0.6%.

3.2 The Frequency Diversity

In this section, we fix the observation point at which the incident angle is $\theta = 0^\circ$. The frequencies $f = 100 + 10i(MHz), i = 0...9$ are chosen at first. Then the frequencies $f = 500 + 10i(MHz), i = 0 \cdots 9$, which belong to the resonance band according to the electrical size and $f = 1\,(GHz) + 10i\ (MHz), i = 0, \cdots 9$, which belong to the optical band are chosen. The wind speed is taken as $U = 0m/s$.

The average errors are shown in Table 1. When the incident wave frequencies are raised up, the average errors of the reconstruction get higher. This unsatisfactory reconstruction results could be an effect of the different scattering characteristics in different frequency bands.

Table 1: Relative errors in the reconstruction.

Frequency (MHz)	Average	Maximum	Minimum
100-190	0.1%	0.3%	0.05%
500-590	2.1%	3.9%	0.06%
1000-1090	4.4%	8.4%	0.8%

In order to investigate the scattering characteristics in resonance and optical bands, we fix the frequency at $f = 300MHz$ and $f = 1GHz$ respectively and change the square side length according to the rule: $L = 4.01 + 0.1i\ (m) i = 0, \cdots 39$. The results are shown in Figure 2 and Figure 3.

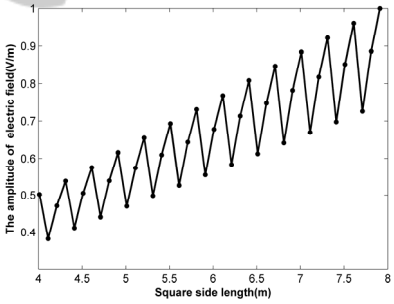

Figure 2: The characteristic of scattered fields in optical band.

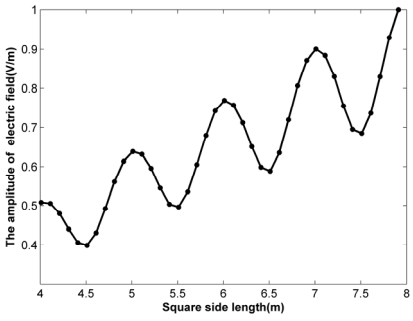

Figure 3: The characteristic of scattered fields in optical band.

As shown in the figures above, the scattered electric fields in the optical band are characterized by an acute oscillating profile while the one in the resonance band is changing much more gently. In order to overcome this problem, much more square samples are needed. Figure 4 reports the amplitude of electric fields for $f = 1GHz$ with square side lengths changing according to the rule: $L = 4.01 + 0.03i\ (m)\ , i = 0, \cdots 132.$ The observation point is still the one with incident angle $\theta = 0^{\circ}$.

In Figure 4, the accurate relationship between the amplitude of the backscattered electric field and square side length can be established and the profile is oscillating much more gently. Actually, when the number of square samples is increased, the geometric information carried by the electric fields are more completed and integrated which is beneficial to the inverse scattering procedure.

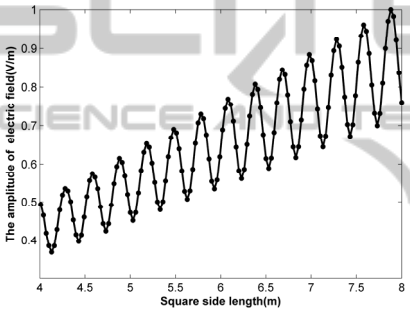

Figure 4: The characteristic of scattered files in optical band with more samples.

The analysis above gives us a hint on how to improve the reconstruction results in optical band. We redo the optical case with a new training set: $L = 4.01 + 0.015i\ (m)\ , i = 0, \cdots 59$. The other computational parameters are kept the same. Now, the reconstruction results are with an average error less than 1% .

As can be argued from the above experiments, in order to get an satisfactory reconstruction result, more training samples are usually needed for the optical band.

However, in these examples, the observation point has been fixed at which the incident angle is $\theta = 0^{\circ}$. In the section followed, we choose different observation points to discuss how the spatial diversity affects the reconstruction.

3.3 The Spatial Diversity

In this section, the role of the spatial diversity in the reconstruction is investigated by means of changing the observation points.

At first, The incident wave frequencies are chosen according to the rule $f = 300 + 10i\ (MHz), i = 0, \cdots 9.$ Then, three different observation points with incident angle $\theta = 22^{\circ}$, $\theta = 45^{\circ}$, and $\theta = 70^{\circ}$ respectively are chosen to gather backscattered fields. The training and test sets are the same as we used in 3.1. The wind speed is taken as $U = 0m/s$.

The average errors with respect to the three observation points are shown in Table 2. It is easy to find that when the incident angle is $\theta = 45^{\circ}$, we can retrieve the square side lengths accurately. This phenomenon may have relations to the dihedral corner reflector consists of the square edge and the bottom surface. We can fix the frequency at $f = 1GHz$ and set the incident angle $\theta = 45^{\circ}$ to investigate how the electric fields vary in terms of the square side lengths. The square side lengths selected are changing according to the rule: $L = 4.01 + 0.1i\ (m), i = 0, \cdots 39$. The results are showed in Figure 5. It is interesting to find that the scattered electric fields are changing much more gently and linearly when the observation point is set at the one with incident angle $\theta = 45^{\circ}$. The special scattering characteristics of the dihedral corner reflector are beneficial to the inverse scattering procedure, which implies the nonlinear regression is close to a linear one.

Table 2: Relative errors in the reconstruction.

Incident Angle	Average	Maximum	Minimum
22°	3.1%	6.9%	0.6%
45°	0.1%	0.3%	0.003%
70°	3.4%	6.2%	0.2%

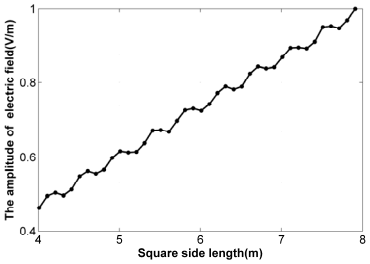

Figure 5: The characteristic of scattered fields.

In section 3.2, when the incident angle is $\theta = 0^{\circ}$, we fail to retrieve the square side length in optical band with the same training set used in resonance band. The reconstructed results are improved by increasing the number of training samples, which obviously raises the burden of making training set. What's worse, the SVM needs more time to do the regression. The above numerical simulation results

tell us that when the incident angle is $\theta = 45^{\circ}$, it is easier to get an satisfactory reconstruction results due to the strong interaction of the dihedral corner reflector. So, in the following , we will try to retrieve the square side length when the training and test set are kept the same as we used in resonance band as $L = 4.01 + 0.1i(m), i = 0,\cdots 9$ and $L = 4.045 + 0.1i(m), i = 0 \cdots 8$ respectively. However, the observation point with $\theta = 45^{\circ}$ will be used instead of the one with $\theta = 0^{\circ}$. The wind speed is taken as $U = 0m/s$.

The reconstruction results with an average error less than 1% which means the square side lengths are accurately reconstructed for optical band with the same training set as we used in resonance band.

3.4 Reconstruction in Multifrequency–Singleview-Monostatic Way

In this section, the bottom surface is a rough surface. Because of the roughness of the bottom surface, more observation points are often needed to capture the special scattering characteristics of the dihedral corner reflector consists of the square edge and the bottom surface. In addition to the side length, the height of the square above the surface is retriev- ed.

The values of L considered during the training phase are $L = 4.01 + 0.05i(m), i = 0...19$, while the height $H = 7.01 + 0.01i(m), i = 0...9$.

The test set is obtained by setting the square side length as $L = 4.045 + 0.1i\ (m), i = 0 \cdots 8$, and the height are set as $H = 7.015 + 0.01i(m), i = 0...8$. The incident wave frequencies are chosen as: $f = 200 + 10i\ (MHz), i = 0...9$. The wind speed is $U = 3m/s$.

The relative errors with observation points set at $\theta = 42^{\circ}, 45^{\circ}$ and 48° are shown in Table 3. Both the side length and height are retrieved accurately. The relative errors reconstructed with 21 observation points set equally along the measurement line are shown in Table 4 for a comparison.

From Table 3 and Table 4, it is interesting to find that the errors are almost the same and sometimes the one reconstructed with more observation points has slightly higher errors. That is to say, more observation points do not guarantee a better reconstruction results. As a second remark, more observation points consume much more computational resources.

Table 3: Relative errors of side length and height for 3 observation points.

	Average	Maximum	Minimum
RelErr(H)	0.05%	0.17%	0.0003%
RelErr(L)	0.11%	0.33%	0.001%

Table 4: Relative errors of side length and height for 21 observation points.

	Average	Maximum	Minimum
RelErr(H)	0.06%	0.17%	0.0001%
RelErr(L)	0.12%	0.39%	0.001%

4 CONCLUSIONS

In this paper, we investigated the geometric parameters reconstruction of an electrically large square above the rough surface. The role of the spatial and frequency diversity in the reconstruction is investigated in detail with respect to the characteristics of the scattered field. At last, the side length and height of the square above the rough surface are retrieved accurately with the backscattered multifrequency data collected at just a few observation points which are specially selected based on the scattering characterisitics.

REFERENCES

H. X. Ye, Y. Q. Jin., 2006. Fast iterative approach to difference scattering from the target above a rough surface. *IEEE Press.*

F. S. Deng, S. Y. He, H. T. Chen, W. D. Hu, W. X. Yu, G. Q. Zhu., 2010. Numerical Simulation of Vector Wave Scattering From the Target and Rough Surface Composite Model With 3-D Multilevel UV Method. *IEEE Press.*

S. Caorsi, G. Cevini., 2005. An electromagnetic approach based on neural networks for the GPR investigation of buried cylinders. *IEEE Press.*

E. Bermani, A. Boni, S. Caorsi, A. Massa. An innovative real-time technique for buried object detection. *IEEE Press.*

R. Firoozabadi, E. L. Miller, C. M. Rappaport, A. W. Morgenthaler., 2007. Subsurface Sensing of Buried Objects Under a Randomly Rough Surface Using Scattered Electromagnetic Field Data. *IEEE Press.*

E. Bermani, S. Caorsi, M. Raffetto., 2000. Geometric and dielectric characterization of buried cylinders by using simple time-domain electromagnetic data and neural networks. *Wiley Press.*

E. Pettinelli, A. D. Matteo, E. Mattei, l. Crocco, F. Soldovieri, J. D. Redman, A. P. Annan., 2009. GPR Response From Buried Pipes: Measurement on Field Site and Tomographic Reconstructions, *IEEE TePress.*

Q. H. Zhang, B. X. Xiao, G. Q. Zhu., 2007. Inverse scattering by dielectric circular cylinder using support vector machine approach,. *Wiley Press.*

A. Qing., 2003. Electromagnetic inverse scattering of multiple two-dimensional perfectly conducting objects by the differential evolution strategy. *IEEE Press.*

V. Vapnik., 1998. Statistical Learning Theory. *Wiley Press. New York*